# The Colorado Wind-Profiling Network

R. G. STRAUCH, D. A. MERRITT, K. P. MORAN, K. B. EARNSHAW AND D. VAN DE KAMP

*NOAA/ERL/Wave Propagation Laboratory, Boulder, CO 80303*

(Manuscript received 18 August 1983, in final form 23 November 1983)

ABSTRACT

Remote sensing instrumentation has advanced to the point where serious consideration is being given to a next-generation tropospheric sounding system that uses radars and radiometers to provide profiles of tropospheric variables continuously and automatically. A network of five wind-profiling radars has been constructed in Colorado. This network represents a significant step in the development of a new observing system for operational and research meteorology. The radars and their capabilities and limitations are described.

## 1. Introduction

Vertical profiles of the horizontal wind can be measured throughout the troposphere in nearly all weather conditions with VHF and UHF Doppler radars. This capability is being exploited in research systems and is being considered for operational applications. For example, a national network of wind-profiling radars has been proposed for fuel-efficient flight planning for commercial aviation (Carlson and Sundararaman, 1982); it is projected that such a network could save several hundred million dollars annually in fuel costs.

The Wave Propagation Laboratory (WPL) is developing a ground-based remote sensing system to measure tropospheric wind, temperature and humidity; the prototype version of this system (called Profiler) uses radars at 0.33 and 6 m wavelengths to measure winds (Hogg *et al.*, 1983). There are five radar wind Profilers currently operating continuously and unattended in Colorado. Data from this network are being used for real-time testing of improved forecast methods and for mesoscale research. The data are also being evaluated by aviation weather forecasters. Long-term operation of these radars will help answer questions concerning the type of radar best suited for an operational network. These questions include the choice of radar wavelength, the radar sensitivity required, methods of averaging for representativeness and the economics of the system.

The application of radar to operational wind profiling is described by Balsley and Gage (1982); the WPL Profiler is described by Strauch *et al.* (1983). One objective of the Profiler program is to develop tropospheric wind-profiling radars that will

- provide vertical profiles of the horizontal wind throughout the troposphere,
- operate in nearly all weather conditions,
- provide wind data automatically and continuously with unattended operation,
- be suitable for widespread use in networks,
- provide data for mesoscale and synoptic scale applications.

Measurement objectives have evolved from discussions with meteorologists and experience with research radar systems. The goal is to provide vertical profiles of the horizontal wind with

- accuracy of orthogonal components to better than 1 m $s^{-1}$;
- height resolution of 100 m below 600 mb, 300 m to 300 mb, and 1 km to 100 mb;
- temporal resolution of 15 min for profiles to 600 mb, 30 min for profiles to 300 mb, and 60 min for profiles to 100 mb.

This paper describes the five Colorado wind profiling radars, the method used to measure winds, the data processing and averaging, data outputs and automated operation.

## 2. Method of wind measurement

Sensitive VHF or UHF radars are needed to measure winds in optically clear air; sensitivity is achieved through the use of large-aperture antennas, high average power, low-noise receivers and long-time integration. The Colorado wind-profiling radars all use fixed pointing antennas with two or three pointing directions; this avoids the costs and complexities of large mechanically or electronically steered antennas. Three antenna beam-pointing directions are needed to measure the vector wind; for simplicity the pointing directions are chosen to observe orthogonal horizontal wind components $u$ and $v$, and the vertical component $w$. Horizontal winds are measured with an antenna elevation pointing angle $\theta_e$ that allows observation at all altitudes of interest.

The radial Doppler velocities $V_i$ measured by the radar are related to the wind as follows:

$$V_1 = u\cos\theta_e + w\sin\theta_e,$$

$$V_2 = v\cos\theta_e + w\sin\theta_e,$$

$$V_3 = w,$$

where the antenna azimuth angles for $V_1$ and $V_2$ are 0° and 90°, respectively. At each altitude $h$ the three measurements are made at volumes separated in space. Horizontal uniformity is assumed when the measurements are combined. Two types of error can result from this assumption: first, $u$ and $v$ measured at the observation volume will be in error by $h\Delta w/\Delta x$ and $h\Delta w/\Delta y$, respectively; and second, the measured $u$ and $v$ will differ from the $u$ and $v$ directly above the radar by $(\Delta u/\Delta x)h\cot\theta_e$ and $(\Delta v/\Delta y)h\cot\theta_e$, respectively. Note that these two error or bias terms are fundamentally different; gradients of $w$ cause errors in the wind measurement whereas gradients of $u$ and $v$ do not cause errors at the measurement points. They cause "errors" only when the measurement point is translated to the radar location. This latter type of "error" is also present in conventional balloon wind soundings unless it is recognized that the measurements do not apply to the launch site. These "errors" can be large for balloon soundings because of the large displacement that can occur, particularly at upper levels or in high winds. With balloon soundings both horizontal wind components are measured at the same location, which varies with height and time; fixed-beam radars measure the wind components at different locations, which depend on height but remain fixed. The importance of horizontal gradients of $u$ and $v$ in radar-measured winds depends on the application. For example, if data from a network of radars are to be interpolated onto a rectangular grid, the actual location of the observation volume could be used and there would be no error caused by these gradients. On the other hand, horizontal gradients of $w$ cause errors at the observation points and these errors limit the accuracy of horizontal wind measurements with Doppler radar.

It is commonly assumed that in the optically clear atmosphere horizontal winds can be measured with just two antenna pointing directions if averaging times are sufficiently long that $w$ can be ignored. In some clear-air cases, e.g., near strong convection or when waves are present, vertical motions cannot be ignored. In such cases, horizontal gradients of $w$ render the additional information provided by a zenith measurement of $w$ of questionable value. No single device (Doppler or balloon) can measure meaningful wind profiles in complex meteorological regimes. During precipitation the measured Doppler velocity spectra may be caused by a combination of scattering from refractive turbulence and hydrometeors. Hydrometeors generally trace the mean wind but also may have fallspeeds as large as 9 m s$^{-1}$ [even larger for hail, Atlas *et al.* (1973)]. The hydrometeor scattering signal can be stronger than the signal from refractive turbulence, even for VHF radars. However, VHF radars rarely observe precipitation, possibly because the minimum height of observation is often above the freezing level. We therefore ignore precipitation for our Colorado VHF radars and use just two pointing directions with long-time (~1 h) averaging to minimize the effects of vertical air motion on the horizontal wind measurements. UHF radar scattering will be from hydrometeors rather than clear air during precipitation; the transition from scattering by refractive turbulence to scattering by hydrometeors occurs for small particles with low fallspeeds. Therefore, individual Doppler spectra will rarely show the bimodal velocity distribution of the two types of scattering. Our UHF radar has three pointing directions so that corrections for fall-speeds can be made in stratiform precipitation.

All five Profiler radars (four VHF and one UHF) use elevation angles of 75° to measure the horizontal wind. The choice of elevation angles is dictated by conflicting requirements. An elevation angle of 75° represents an acceptable compromise between various requirements. The following factors dictate use of the highest possible elevation angles:

1) If the physical axis of the antenna is directed toward the zenith (the usual case for large phased arrays or large fixed reflectors) the elevation pointing angle should be as high as possible to keep the effective aperture nearly the same as for zenith pointing. The loss in sensitivity varies as $\csc\theta_e$ and is 0.15 dB for a 75° elevation angle.

2) The elevation pointing angle should be as high as possible to minimize the range to a given height. The range is $h/\sin\theta_e$, and the loss in sensitivity varies as (range)$^2$. This loss is 0.3 dB for a 75° elevation angle.

3) The height resolution of the radar depends on the range resolution and the cross-beam dimensions of the antenna illumination. The antenna elevation angle should be high enough that the height resolution will not be degraded by cross-beam resolution at the highest altitude of interest. We want radar range resolution $\Delta R$ to determine height resolution because range resolution is controllable by system bandwidth whereas cross-beam resolution is fixed by antenna dimensions. Thus, the cross-beam dimension $h_m\beta_2\cot\theta_e$ should be less than $\Delta R\sin\theta_e$, where $h_m$ is the maximum height of interest and $\beta_2$ is the two-way antenna beamwidth. At an elevation angle of 75° the cross-beam height dimension is less than 500 m at 20 km altitude for two-way antenna beamwidth of less than 5°.

4) The elevation angle should be as high as possible to minimize the effects of wind gradients discussed earlier.

5) The elevation angle should be as high as possible for antennas whose physical axis points toward zenith

so that off-axis antenna patterns are not unduly degraded.

Opposing these factors that mandate elevation angles near zenith are those that dictate lower elevation angles:

1) The elevation angle should be as low as possible to produce accurate wind measurements because uncertainty in the measurement of radial velocity causes an uncertainty in horizontal wind that increases with elevation angle. If vertical velocities are neglected,

$$\text{STD DEV}(\hat{u}, \hat{v}) = [\text{STD DEV}(\hat{V}_i)] \sec\theta_e,$$

where the circumflex denotes an estimated quantity. Our ability to obtain unbiased estimates of $V_i$ with low standard deviation depends on radar wavelength, signal-to-noise ratio, observation time, and the width of the Doppler spectrum (Zrnic, 1979). We want to obtain estimates at low signal-to-noise ratios where STD DEV ($\hat{V}_i$) may be 1 m s$^{-1}$ or more for individual observations. If we derive average horizontal winds from $N$ independent observations with an uncertainty of 1 m s$^{-1}$, then $\sec\theta_e$ must be at most $\sqrt{N}$ if the individual radial measurements have an uncertainty of 1 m s$^{-1}$. For radars that obtain hourly wind averages from 15 observations, the elevation angle should not be greater than 75°.

2) Bias errors in the wind measurements caused by errors in antenna pointing direction increase with increasing elevation angle. If the antenna pointing is in error by 10% of the beamwidth, a value that should be achieved in practice with a nonsteerable antenna, the bias will be less than 3.6% for beamwidths less than 5° and elevation angles less than 75°.

3) At long wavelengths (>3 m) enhanced radar reflections are observed with a zenith-pointing beam. These reflections are caused by horizontally stratified atmospheric layers; their intensity decreases as the antenna elevation angle decreases from zenith. However, if the antenna is pointed too close to zenith, the effective pointing angle will be biased toward zenith, and this pointing error will bias wind measurements toward low values. At 15° off zenith, this effect should be negligible (Röttger, 1980).

## 3. Data processing and averaging

All five wind profiling radars are coherent pulse Doppler radars and all use the data processing scheme illustrated in Fig. 1. Radial profiles of the first three moments of the Doppler spectra are estimated: signal power $P$, mean radial velocity $V_r$ and spectrum width $W$. The input signal is the backscattered signal for each radar resolution cell after translation to a convenient frequency. The receiver limits the bandwidth with a filter that is matched to the transmitted pulse. Complex video is obtained by baseband mixing with a reference voltage. Video voltages are measured for each pulse repetition period $T$ and for each range resolution cell centered along the antenna axis; these voltages represent the composite amplitude and phase of the scattering process in the resolution volume. The averaging that occurs in each step of the data processing is examined below.

The signal-to-noise ratio (SNR) can be improved for wind-profiling radars by summing the complex video samples from a number $J$ of consecutive received pulses. Since the noise bandwidth is determined by the radar pulse width, noise samples taken at the pulse repetition period will be uncorrelated; therefore the noise power increases linearly with the number of samples added. The signal, however, remains well correlated for approximately $0.2\lambda/W$ seconds (Nathanson, 1969), where $\lambda$ is the radar wavelength. Typically $W$ is $\sim$1 m s$^{-1}$, so the correlation time is milliseconds with microwave radars and seconds with VHF radars. If, in addition to being correlated, the phase of the signal samples changes very little between samples, then signal samples can be added so that signal power increases with the square of the number of samples added. This occurs for radars whose unambiguous velocity $\lambda/(4T)$ is much greater than the radial velocity of the scatterers. The SNR improves by the number $J$ of samples averaged, and the unambiguous velocity decreases to $\lambda/(4JT)$.

Three points should be noted in regard to signal averaging. 1) It is not necessary to use time domain averaging to improve detection. The SNR improvement can be obtained in later processing, but time domain averaging minimizes the calculation burden in succeeding processing stages without sacrificing sensitivity. 2) Time-domain averaging filters the input signal so that signal components with velocity greater than $\lambda/(4JT)$ will be aliased and attenuated (Schmidt *et al.*, 1979). Without time-domain averaging, when signal components are aliased they are not attenuated. 3) It is possible to select $J$ and $T$ such that interference at particular frequencies is virtually eliminated. For the 6 m wavelength radars we select $J$ and $T$ so that 60 Hz is rejected as shown in Fig. 2. We select $J$ as large as possible such that $\lambda/(4JT)$ is greater than the

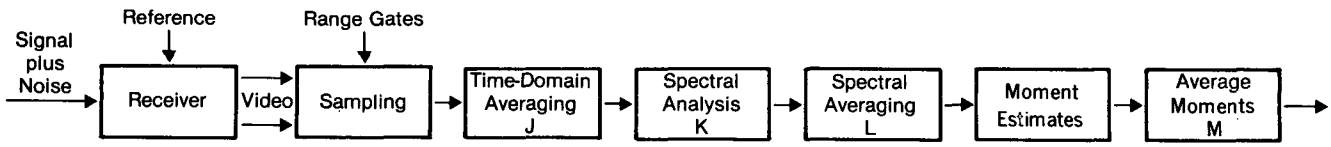


FIG. 1. Data processing steps for wind profiling Doppler radars.

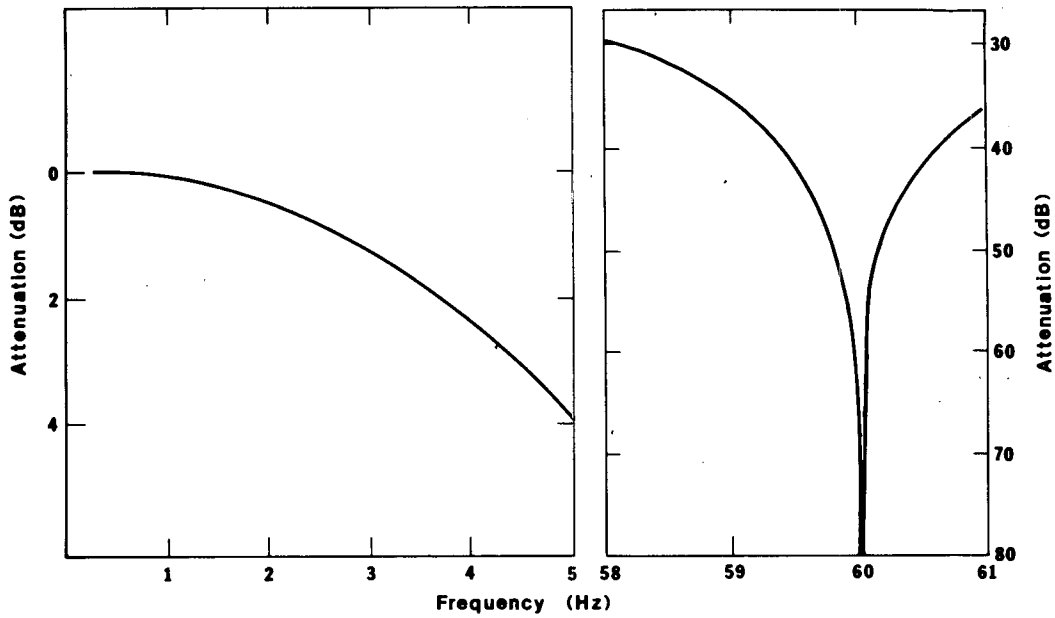


FIG. 2. Filter response for time-domain integration of video samples. The Nyquist frequency is 5 Hz. Pulse repetition period and the number of time-domain averages are selected to attenuate 60 Hz.

maximum expected mean radial velocity and such that the signal is correlated for much longer than $JT$.

The next step in signal processing is to compute the power spectrum of $K$ (averaged) signal samples. We select $K$ such that the achievable coherent integration is realized. If $K$ is too small, sensitivity is reduced; if $K$ is too large, the calculation burden is increased without improving sensitivity or retrieving additional information. Fig. 3 shows how the SNR in the spectral domain improves as dwell time $T_D = JKT$ increases. The improvement factor is given by

$$K\text{erf}(\Delta V/2\sqrt{2W}),$$

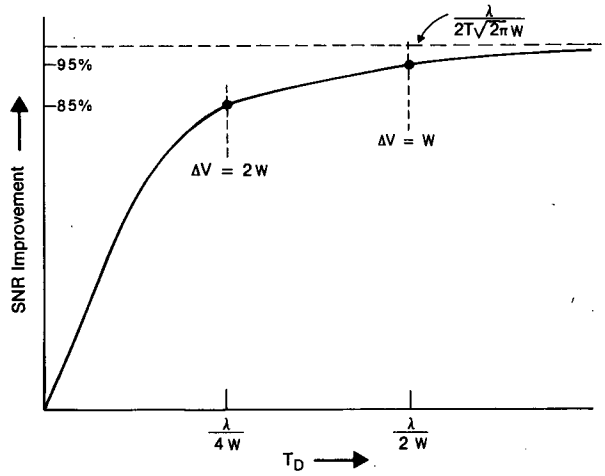


FIG. 3. Signal-to-noise ratio improvement from spectral processing. Coherent integration achieved with spectral processing is limited by the coherence time of the scattering process.

where $\Delta V$ is the velocity resolution of the spectral processor $\lambda/(2T_D)$. For small $K$ the improvement factor increases linearly with $K$; spectral resolution is so poor that all the signal power remains in one velocity resolution element. As observation time increases, the noise power in each velocity resolution element decreases, while signal power remains constant. When the dwell time is increased to the extent that signal power starts to occupy more than one spectral point, SNR improvement no longer increases linearly with dwell time. When the dwell time is $\lambda/(2W)$ or $K = \lambda/(2JTW)$, 95% of the achievable coherent integration is achieved. Longer dwell times yield little SNR improvement because both noise power and signal power decrease in the velocity resolution element that contains maximum signal. Note, however, that for large $K$, spectral points can be averaged and the spectrum will still be resolved. If this is done, SNR improves as $T_D^{1/2}$ as expected for incoherent integration. Thus, to minimize calculations we choose $K \doteq \lambda/(2JTW)$ and use any additional observation time to measure new spectra.

The next processing step is the averaging of $L$ spectra, each obtained from $JK$ radar pulses. The $L$ power spectral density estimates for each frequency or velocity will be exponentially distributed with a standard deviation equal to the mean (Hildebrand and Sekhon, 1974). We expect averaging to improve the spectral domain SNR by $\sqrt{L}$; however, this improvement will occur only if the mean wind is the same for each dwell time. If the mean wind is not the same, then the width of the averaged spectrum increases during the averaging and the SNR improvement will be less than $\sqrt{L}$. It is

readily seen that if the mean wind changes abruptly by more than $W$, then the SNR can actually decrease with averaging time. The dependence of spectral width on averaging time can be deduced by examining the dependence of spectral width on averaging distance as studied by Frisch and Clifford (1974) and Labitt (1981). They derive the relationship $W \propto d^{1/3}$ where $d$ is the maximum dimension of the observation volume (beamwidth or range resolution, whichever is greater) and $d$ is less than the outer scale of turbulence $L_0$. If we average for time $T_0$ such that $d < \bar{v}T_0 < L_0$, then, using Taylor's hypothesis, $W \propto (\bar{v}T_0)^{1/3}$ where $\bar{v}$ is the mean wind speed. Therefore, if the averaging time is less than $d/\bar{v}$, then the width of the averaged spectrum is about the same as the width of the individual spectra; for greater averaging time, the width of the averaged spectrum increases as $T_0^{1/3}$. To take full advantage of $\sqrt{L}$ improvement in SNR by averaging spectra, $L$ should be limited to about $d/(JKT\bar{v})$.

Next, we estimate the important spectral moments from the averaged Doppler velocity spectrum. The signal spectrum must be isolated from the measured signal-plus-noise spectrum before the moments can be found. The methods used to do this (and to remove undesired spectral components such as ground clutter near zero velocity) are as follows (Carter, 1982). First, the average value of the complex time series is removed prior to calculating the power spectrum to eliminate any fixed clutter or DC offsets in the signal channel. Next, the mean noise level is found by applying an objective technique (Hildebrand and Sekhon, 1974) for each spectrum. A fixed noise level cannot be assumed for the 6 m wavelength radars because the noise is governed by cosmic background. The signal spectrum is isolated by locating the peak value of the averaged spectrum and including all those contiguous spectral points that exceed the noise level. The classical definition of the moments is then applied to the isolated signal spectrum after subtracting the mean noise level from each of the selected spectral points. In very weak signals, or if the input consists of noise only, the algorithm selects the peak and adjacent spectral points; it therefore becomes a maximum likelihood estimator of the mean velocity (Whalen, 1971). It is an unbiased estimator of the mean velocity [in noise it selects a random value between $(\pm\lambda/(4JT)]$. Since it selects that portion of the noise in the isolated spectral points that exceeds the mean noise as "signal", both power and width estimates are biased by the noise. This method appears to work well for a wide variety of conditions. Fig. 4 illustrates how the spectral moments are derived from the Doppler spectra.

Finally, estimates of spectral moments can be averaged. The averaging time depends on the type of information sought and the temporal evolution of the scattering phenomena and meteorology. For example, the 6 m wavelength radars are used primarily to obtain hourly estimates of tropospheric winds; during 1 h, $M$ radial profiles of mean velocity are measured for each orthogonal wind component. At the upper heights the mean velocities are sometimes random because of low SNR. Some of the profiles are also contaminated by interference from other transmitters or by scattering from aircraft. The radial velocity profiles are averaged by applying a simple version of random sample consensus (Fischler and Bolles, 1981). The set of $M$ data points at each measurement height is examined to find the largest subset of points within $X$ m s$^{-1}$ of each other. If the subset includes fewer than $Y$ data points, the data are rejected for that height; otherwise the subset is averaged to obtain the mean radial wind. This algorithm rejects data when the SNR is too low and also rejects random points caused by aircraft interference. In practice $X$ is 1–2 m s$^{-1}$ (where the maximum radial velocity is about 18 m s$^{-1}$), and the smallest subset allowed is 4 of 11 or 12 measurement points.

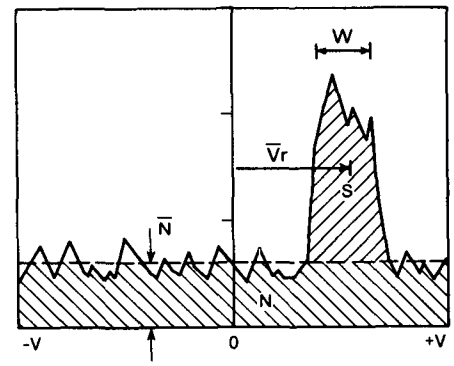


FIG. 4. Derivation of spectral moments from Doppler spectra for wind-profiling radars. $\bar{N}$ is the noise level, $N$ the total noise power, $S$ the signal power, $V_r$ the mean radial velocity, and $W$ the width of the spectrum.

## 4. Radar characteristics

Fig. 5 shows the location of the five Colorado wind-profiling radars. These sites were selected by research meteorologists concerned with weather forecasting for metropolitan Denver. Profilers at these sites make possible continuous monitoring of winds in major weather systems that affect Denver. The 6-m-wavelength radar at Platteville was originally developed by NOAA's Aeronomy Laboratory (AL) and is being operated jointly by AL and WPL. The 6 m wavelength radars near Sterling, Craig and Cortez are similar in technology to the Platteville radar. The 33 cm radar is located at the main Profiler site near the National Weather Service Forecast Office at Denver's Stapleton International Airport. Data from the four VHF radars are transmitted by telephone to the central Profiler computer. A brief description of the radars follows.

### *a. The 6 m radar at Platteville*

The radar at Platteville has been described by Ecklund *et al.* (1979). It has operated continuously and

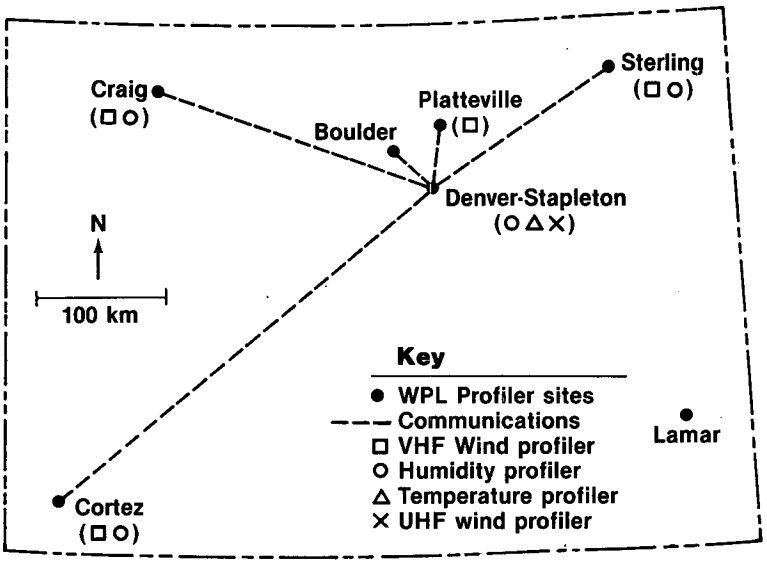


FIG. 5. Wind profiling radar sites in Colorado. Temperature and humidity profilers are currently installed at Denver-Stapleton.

unattended since mid-1981, except for brief periods of downtime caused by computer problems. Since January 1982 data have been tape recorded routinely.

The radar alternates between two modes of operation: one for measuring vertical profiles of the horizontal wind, and the other for zenith-pointing observations. Each mode is used every 5 min; following *each* operation cycle the data are transmitted by telephone to the Profiler computer (24 times per hour) because the computer at the radar site (Data General NOVA-800) is not able to do the total data processing task. There are three antennas, transmitters and receivers, so data are obtained simultaneously in the three viewing directions. Table 1 summarizes the radar characteristics and operating parameters.

The major limitations of this radar are imposed by the data system. A minicomputer performs all the time domain integration in software, and this restricts the maximum pulse repetition frequency, the minimum spacing of range gates, and the number of range gates allowed. As a result the radar is operated with coarse range resolution and relatively poor minimum height coverage (~2 km above ground). The data system also limits sensitivity by restricting the duty cycle. There are 13 range cells for monitoring winds in the troposphere and 10 range cells for monitoring mesospheric echoes. Present plans are to replace the data system with a more versatile system that includes a preprocessor (used with the four radars described below) and to replace the two off-zenith antennas that are not as efficient as newer antennas because of losses in the cables used for the dipole arrays. A minicomputer is used for data processing (including spectral analysis), so the number of range cells would be restricted to about 32 to keep the data processing time small com-

TABLE 1. Platteville radar characteristics and operating parameters.

| *Radar characteristics* | |
|---|---|
| Frequency | 49.92 MHz |
| Authorized bandwidth | 0.4 MHz |
| Peak power | 27 kW (maximum ≈ 60 kW) |
| Average power | 180 W (maximum ≈ 1 kW) |
| Pulse width | 16 μs |
| Pulse repetition period | 2400 μs |
| Antenna aperture | 100 m × 100 m |
| Antenna pointing | zenith, 15° off-zenith to north and east (3 antennas) |
| Antenna type | fixed phased array of colinear-coaxial dipoles |
| Two-way beamwidth | 2.5° |

| *Operating parameters* | Vertical mode | Horizontal-wind mode |
|---|---|---|
| Data processing | | |
| Time domain averaging | 256 pulses | 32 pulses |
| Spectral averaging | 2 | 16 |
| Maximum radial velocity | ±2.44 m $s^{-1}$ | ±19.55 m $s^{-1}$ |
| Spectral resolution (64 points) | 0.076 m $s^{-1}$ | 0.61 m $s^{-1}$ |
| Tropospheric sampling | | |
| First height | 1.85 km | 2.5 km |
| Height spacing | 1.5 km | 1.45 km |
| Number of heights | 13 | 13 |
| Mesospheric sampling | | |
| First height | 67.5 km | 65 km |
| Height spacing | 3.6 km | 3.48 km |
| Number of heights | 10 | 10 |

pared with the acquisition time. Range resolution would then be limited by the bandwidth authorized (400 kHz).

### b. New VHF radars

The VHF radars near Sterling, Craig and Cortez were placed in operation in March, April and May 1983. These radars transmit simultaneously in two pointing directions and have 50 m × 50 m antennas. Computers (Data General Eclipse-120) and data systems perform the complete data analysis at the radar site. Wind profiles are sent by telephone once per hour to the Denver computer. Two resolution modes are used: a 3 μs pulse width for low and middle levels and a 9 μs pulse width to extend the height coverage as high as possible. The data are sampled with 2 and 6 μs gate spacing for the two modes. In the usual sequence of operation, hourly wind profiles are measured using 24 profiles, 12 with each pulse width. The profiles alternate pulse widths and finish the data acquisition cycle in about 45 min. The last 15 min are idle to allow the telephone communication system to poll all the outlying sites and to allow the radar operator to access the station to make changes or obtain diagnostic outputs. The telephone transmission from each site takes about 40 s. Table 2 lists the radar characteristics. Note the unusual pulse repetition periods and number of time domain averages that are selected to reject 60 Hz.

TABLE 2. New VHF radar characteristics and operating parameters.

| *Radar characteristics* | |
|---|---|
| Frequency | 49.8 MHz |
| Authorized bandwidth | 0.4 MHz |
| Peak power | 30 kW (maximum ≈ 60 kW) |
| Average power | 400 W (maximum ≈ 1 kW) |
| Pulse width | 3, 9 μs |
| Pulse repetition period | 238.67, 672 μs |
| Antenna aperture | 50 m × 50 m |
| Antenna pointing | 15° off-zenith to north and east (2 antennas) |
| Antenna type | fixed phased array of colinear-coaxial dipoles |
| Two-way beamwidth | 5° |

| *Operating parameters* | Mode 1 | Mode 2 |
|---|---|---|
| Data processing | 3 μs pulse | 9 μs pulse |
| Time domain averaging | 419 pulses | 124 pulses |
| Spectral averages | 8 | 16 |
| Maximum radial velocity | ±15.7 m s$^{-1}$ | ±19.6 m s$^{-1}$ |
| Spectral resolution (64 points) | 0.49 m s$^{-1}$ | 0.31 m s$^{-1}$ |
| Height sampling | | |
| First height | 1.4 km | 3.0 km |
| Height spacing | 290 m | 870 m |
| Number of heights | 22 | 18 |

```
SITE: FLEMING
DATE:  5  7 83
TIME: 12  0  0
NPRO:  11  NTDA:  419  NOSP:   8  PULH:  3.67  PRPR:  238.67
VMAXH:  58.147
FIRST HEIGHT (KM,AGL):   1.40
# OF HEIGHTS:   22.
DELTA HEIGHT (KM):  .29
RFLC ANT:   1
HT#   HS     HD      HT     #E     #N     RFLC
 1    1.1  255.7    2.7     11     11     56.4
 2    1.2  232.0    3.0     11     11     49.7
 3    2.8  261.5    3.3     11     11     52.3
 4    2.8  285.0    3.6     11     11     53.6
 5    5.0  330.1    3.9     11     10     53.1
 6    9.7  347.3    4.2     11     11     54.0
 7   10.5  355.1    4.5     11     11     52.2
 8   10.7    4.2    4.8     11     11     50.2
 9   10.5    5.4    5.1     11     11     49.8
10   10.1  358.1    5.3     11     11     50.3
11    9.8  347.0    5.6     11     11     47.7
12    8.8  335.3    5.9     11     11     46.2
13    9.2  331.4    6.2     11     11     41.2
14    6.7  313.7    6.5     11     11     38.8
15    7.5  330.9    6.8     11     11     32.1
16    6.8  329.4    7.1     11     11     31.5
17    3.3  340.4    7.4     10     11     28.4
18    2.3   30.6    7.7      9     11     27.2
19    2.4     .8    8.0      8     10     21.8
20    4.0  315.5    8.2     11     11     32.2
21    6.6  321.4    8.5     11     11     34.9
22    7.0  319.6    8.8     11     11     31.9

SITE: FLEMING
DATE:  5  7 83
TIME: 12  1 33
NPRO:  11  NTDA:  124  NOSP:  16  PULH:  9.67  PRPR:  672.00
VMAXH:  69.782
FIRST HEIGHT (KM,AGL):   2.90
# OF HEIGHTS:   18
DELTA HEIGHT (KM):  .87
RFLC ANT:   1
HT#   HS     HD      HT     #E     #N     RFLC
 1   10.1  351.7    4.2     11     11     54.7
 2   10.2  357.9    5.1     11     11     53.5
 3    9.3  344.3    6.0     11     11     49.3
 4    7.5  333.6    6.8     11     11     39.3
 5    4.2  332.5    7.7     11     11     34.5
 6    6.9  324.6    8.6     11     11     38.2
 7   13.4  324.9    9.4     11     11     37.2
 8   20.6  320.7   10.3     11     10     35.8
 9   23.5  314.5   11.2     10      9     33.6
10   25.1  298.0   12.1     10      9     29.1
11   23.9  289.7   12.9      9     10     27.6
12   21.8  288.7   13.8     10     10     25.6
13   20.9  283.2   14.7     10      9     25.4
14   20.9  283.4   15.5      8     10     24.8
15   14.0  239.5   16.4      8      6     24.8
16   14.4  244.2   17.3      7      5     22.9
17 -999.0 -999.0   18.1      1      4   -999.0
18    8.9  227.7   19.0      5      5     19.4
```

FIG. 6. Sample of data transmitted by telephone to Denver from wind profilers near Sterling, Craig and Cortez. Two profiles, overlapping in height coverage and with different height resolutions, are measured each hour.

Figure 6 is a sample of the hourly wind profile data obtained by the Fleming radar (near Sterling). The lower level, higher resolution profile typically has very few data dropouts in the hourly average for the altitudes 2.7 to 9 km MSL. The fifth and sixth data columns list numbers of profiles that passed the consensus test for particular heights. The last column is the signal power on the east/west antenna (non-normalized) averaged from those profiles that passed the velocity consensus test. The width of the Doppler spectrum is also calculated but is not yet being transmitted. A major current limitation of the new VHF radar is the minimum height coverage (Fig. 6): about 1.4 km above

the surface. During the first few months of testing the lower resolution profiles typically extend to 16–17 km MSL for the hourly averages, but frequently they extend to the highest altitude observed (19 km MSL). At high altitudes the number of profiles in the consensus set decreases because of low SNR. In the high resolution mode the consensus set is often equal to the total number of profiles used (11 or 12) so that individual profiles appear the same as the hourly average. High resolution profiles (with no consensus testing) are available every 95 s. Likewise, the low resolution profiles could be available every 130 s. Data are not currently recorded at the radar site so these modes are not used because of the telephone time required to transmit the data. Limited archiving at the radar sites will be available for special experiments.

The new VHF radars are remotely controlled; every control function that an operator would exercise on site can be performed by telephone. This includes changing parameters such as pulse width, pulse rate, averaging and sampling, and changing the sequencing or operating modes. The major limitation is that the radar has only two electronically controlled bandwidths. In these radars the time domain averaging function is performed by a hardware pre-processor so the minicomputer is not burdened by pulse-to-pulse calculations. Power spectral analysis is performed in software with a Fast Fourier Transform (FFT) algorithm. The time needed to acquire all the radar samples for a single spectrum is about 6 s, so a software FFT is suitable because there are a limited number of range gates. The total data acquisition time for 45 min of total operation per hour is 27.3 min. Less than one-half of the "dead-time" is FFT calculation time. The radar transmitters do not operate during the dead-time or during the last 15 min of the hour. The radar controller/pre-processor and the software are identical for the three sites, and similar hardware and software also operate the 33-cm radar at Stapleton Airport.

Some of the outputs available by telephone in real time are illustrated in Figs. 7 and 8. Fig. 7 shows the Doppler spectra for the low altitude mode (an average of eight spectra). The brackets indicate the extent of the signal spectrum, and dots indicate power below the display threshold. Signal power increases 1 dB for each letter (the display saturates at $Z$). Fig. 8 shows the corresponding table of moments derived from the Doppler spectra. This data table is sent from the Platteville radar to the Denver computer 24 times each hour, whereas in the new VHF radars 24 such tables are stored prior to calculation of two averaged wind profiles.

### c. *The 33 cm radar*

The 33 cm radar has been in operation since February 1983, but some functions are not yet implemented. It uses a single transmitter and an off-set paraboloidal antenna with three offset feeds to produce the zenith and oblique pointing directions sequentially (Earnshaw *et al.*, 1982). Table 3 lists characteristics and operating parameters. This radar has three electronically selectable bandwidths; 1, 3 and 9 $\mu$s pulses are transmitted. As in the new VHF radars, range gate spacing is two-thirds of the pulse width. Data processing hardware and software are essentially the same as those described for the new VHF system; printout formats and operator control are identical. The Profiler computer, a Data General Eclipse S-250, also serves as the radar computer. This radar detects clouds and precip-

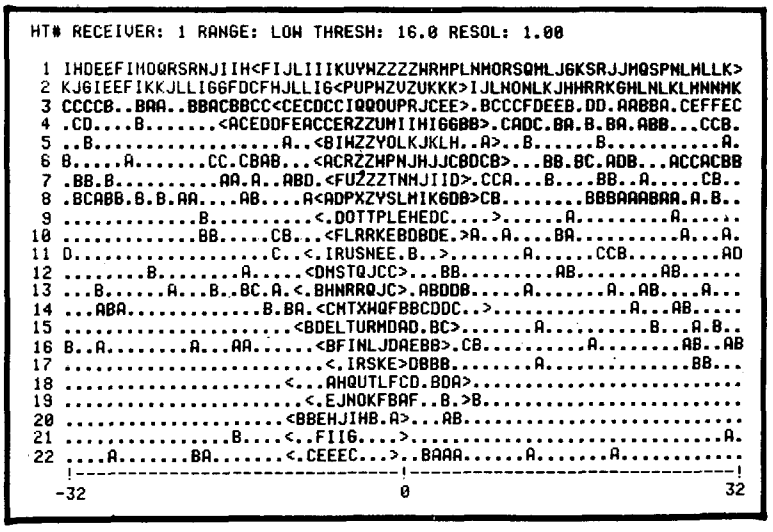


FIG. 7. Sample of real-time Doppler spectra available to a radar operator by telephone.

| HT | DOPPLER M/S | POWER DB | NOISE DB | SIG/NOISE DB | WIDTH M/S |
|---|---|---|---|---|---|
| 1 | 1.4213 | 54.8859 | 20.9754 | 15.8488 | 4.8935 |
| 2 | -.5516 | 49.2716 | 22.3789 | 8.8309 | 1.4730 |
| 3 | -2.3693 | 40.3853 | 17.3375 | 4.9861 | 1.8151 |
| 4 | -5.8489 | 45.8041 | 15.9824 | 11.7599 | 1.3977 |
| 5 | -6.0156 | 50.7871 | 14.8849 | 17.8405 | 1.0275 |
| 6 | -5.6346 | 47.1127 | 15.9015 | 13.1493 | 1.2472 |
| 7 | -5.2704 | 47.6960 | 15.6406 | 13.9936 | 1.2321 |
| 8 | -4.9424 | 46.6131 | 16.1308 | 12.4206 | 1.1627 |
| 9 | -5.6409 | 39.9613 | 14.1256 | 7.7739 | 1.3944 |
| 10 | -6.0717 | 37.2356 | 14.3251 | 4.8487 | 1.4548 |
| 11 | -8.6202 | 39.4990 | 14.0272 | 7.4100 | 1.0775 |
| 12 | -9.4143 | 38.9730 | 14.6850 | 6.2263 | .9605 |
| 13 | -7.8168 | 38.1478 | 15.1027 | 4.9834 | 1.1116 |
| 14 | -6.5963 | 43.0716 | 14.8413 | 10.1685 | 1.1112 |
| 15 | -7.3267 | 40.2745 | 14.4995 | 7.7132 | 1.1567 |
| 16 | -6.0222 | 33.1189 | 14.8800 | .1770 | 1.5202 |
| 17 | -6.0960 | 36.8180 | 14.4863 | 4.2699 | .7055 |
| 18 | -6.6704 | 40.0887 | 14.2663 | 7.7605 | 1.1852 |
| 19 | -7.3745 | 34.5731 | 14.1467 | 2.3646 | 1.7162 |
| 20 | -10.4946 | 30.0539 | 14.1623 | -2.1702 | 1.5289 |
| 21 | -11.5843 | 28.9619 | 13.3643 | -2.4641 | 1.1757 |
| 22 | -12.7501 | 24.8886 | 14.3075 | -7.4807 | 1.2767 |

FIG. 8. Doppler spectral moments derived from the spectra shown in Fig. 6.

itation, so correction for hydrometeor fallspeeds is needed; zenith pointing modes are not currently implemented so low-level data are not valid during precipitation. A second remaining task is to reduce the minimum height for the 1 $\mu$s pulsewidth mode. This will require software additions for clutter suppression at the lowest heights.

One limitation of this system is that the data processing time exceeds the data acquisition time. The wavelength and (therefore) the time needed to acquire the data for a single spectrum are one-eighteenth those of the VHF radars. The software FFT calculation time for the 33 cm radar exceeds the dwell time, thereby reducing the effective observation time. Possible solutions to this problem, such as the use of array processors, are under study.

A more fundamental limitation relating to radar wavelength may be the radar's inability to obtain wind measurements at altitudes above 10 km; turbulent scales measured by clear-air radars may not be in the inertial subrange of turbulence above 10 km. If the $\lambda/2$ scale sizes are in the inertial subrange then the clear-air radar reflectivity is given by $0.38C_n^2\lambda^{-1/3}$ where $C_n^2$ is the refractive index structure constant and $\lambda$ is the radar wavelength (Ottersten, 1969). However if $\lambda/2$ turbulent scales are damped by viscosity then radar reflectivity decreases abruptly as shown by Hill (1978). Fig. 9 shows how the cutoff of radar reflectivity varies with altitude for various levels of mechanical turbulence. For years it has been noted that high-power 10 cm radars measure a sharp decrease in clear-air radar reflectivity above the convective boundary layer. These radars observe elevated layers on occasion. Fig. 9 suggests the reason that 10 cm wavelength Doppler radars can measure low-level winds but are not suitable for routine clear-air wind profiling above about 5 km MSL. It appears that a radar with 33 cm wavelength will also be limited in height coverage. Our early results show that wind profiles can usually be measured to 10 km

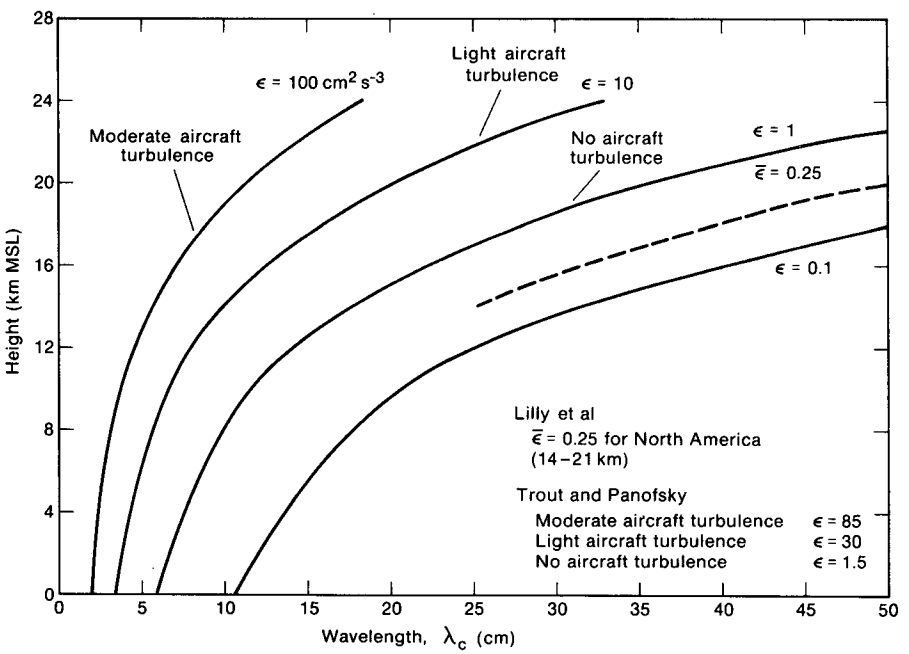


FIG. 9. Cutoff wavelength ($\lambda_c$) vs. height for various levels of mechanical turbulence ($\epsilon$). Routine clear-air wind profiling should be possible with radar wavelengths greater than $\lambda_c$, i.e., to the right of the curves.

TABLE 3. Stapleton radar characteristics and operating parameters.

| *Radar characteristics* | |
|---|---|
| Frequency | 915 MHz |
| Maximum bandwidth | 2 MHz |
| Peak power | 5.6 kW |
| Duty cycle | <25% |
| Antenna aperture | ≈10 m × 10 m |
| Antenna pointing | zenith, 15° off-zenith to north and east |
| Antenna type | offset paraboloidal reflector with offset horn feeds |
| Two-way beamwidth | 1.7° |
| System noise temperature | 240 K |

| *Operating parameters* | Mode 1 | Mode 2 | Mode 3 |
|---|---|---|---|
| Data processing | | | |
| Pulse width | 1 μs | 3 μs | 9 μs |
| Pulse repetition period | 50 μs | 64 μs | 110 μs |
| Average power | 110 W | 260 W | 450 W |
| Time domain averaging | 136 pulses | 80 pulses | 46 pulses |
| Spectral averaging | 8 spectra | 32 spectra | 32 spectra |
| Maximum radial velocity | ±12.02 m s$^{-1}$ | ±15.97 m s$^{-1}$ | ±16.16 m s$^{-1}$ |
| Spectral resolution (64 points) | 0.376 m s$^{-1}$ | 0.499 m s$^{-1}$ | 0.505 m s$^{-1}$ |
| Height sampling | | | |
| First height | 0.35 km | 1.64 km | 2.7 km |
| Height spacing | 100 m | 290 m | 870 m |
| Number of heights | 24 | 24 | 18 |

MSL with the 33 cm radar. Note from Table 3 that this radar has less sensitivity than many 10 cm Doppler radars that cannot measure wind profiles above the boundary layer. However, coverage above 10 km with the 33 cm radar depends on the particular conditions. We expect to conduct side-by-side comparisons with a 10 cm radar to establish the clear-air radar reflectivity behavior near cutoff.

## 5. Data samples

Figures 10–12 illustrate the time/height wind-profiling capability of the Colorado radars. Fig. 10 shows data from the Platteville radar during the passage of a jet stream and trough axis (Shapiro *et al.*, 1983). The data were 1 h average winds calculated at 20 min intervals from 12-samples-per-hour wind measurements. Vertical resolution of the wind observations was ~1.5 km; the first data level was ~4.16 km (MSL). At the beginning of the observing period (1700–1900 GMT) the Profiler showed southwesterly flow between 4.16 and 15.76 km as the jet and trough (Fig. 10) approached from the west. Maximum wind speeds exceeded 55 m s$^{-1}$ in the layer 9.96–14.31 km, and a wind shear of 35 m s$^{-1}$ was present in the layer 7.06–9.96 km. The time interval between 1900 GMT 1 October and 0300 GMT 2 October contained the most dramatic feature within the time series analysis, for during that interval the upper front passed across the Profiler site. First evidence of the frontal wind shears occurred after 1900 GMT when the 7.06 km velocity decreased in speed from 20 to 13 m s$^{-1}$, and the wind direction became slightly more westerly by 2100 GMT. The subsequent frontal passage at the higher levels (8.51, 9.96, 11.41 and 12.86 km) occurred within a 1.5–2 h interval; speed changes of ~30 m s$^{-1}$ and wind direction shifted ~30°.

Figure 11 illustrates the real-time jet stream monitoring capability of the Colorado radar network. Wind profiles at each radar site are shown for the time when the jet stream was over the Cahone radar. The speed and direction of the jet stream shifted at Cahone as the jet moved; eventually it moved northward and crossed all the radar sites.

Figure 12 illustrates the resolution that can be achieved with the UHF radar at Stapleton Airport. Data were measured during a frontal passage; profiles shown were observed with a 1 μs pulse width to 5 km MSL and with a 3 μs pulse width from 5 to 10 km MSL. Fewer than one-half of the measured data points are plotted. Data were available every 30 min (hourly winds are shown) and only one-half of the available data points below 5 km are plotted.

## 6. Planned improvements

The Colorado wind-profiling network will be operated continuously for an indefinite period to supply wind data for evaluation by operational and research meteorologists and by aviation weather forecasters. The only major improvement needed in the new VHF radars is faster receiver recovery to reduce the minimum observable height to about 0.8 km. This may require a redesign of the transmit/receive switch. Minor software changes will be made as necessary, and a satellite communication system will be tested as an alternative to telephone lines. The Platteville VHF radar data system will be replaced with the system used with the other radars. Platteville also needs new antennas to replace two original arrays, which are not as efficient as those in the other VHF radars.

The Stapleton Airport UHF radar software will be changed to add the vertical beam needed to measure particle fallspeeds in precipitation. This radar's minimum observable height also needs to be improved; in this case the transmit/receive switch is satisfactory, but methods to treat ground clutter in the lowest 1.5 km must be developed.

A transportable wind-profiling radar is being developed at UHF (~400 MHz). It is hoped that the best features of the 50 and 915 MHz radars can be combined at a wavelength where suitable bandwidth

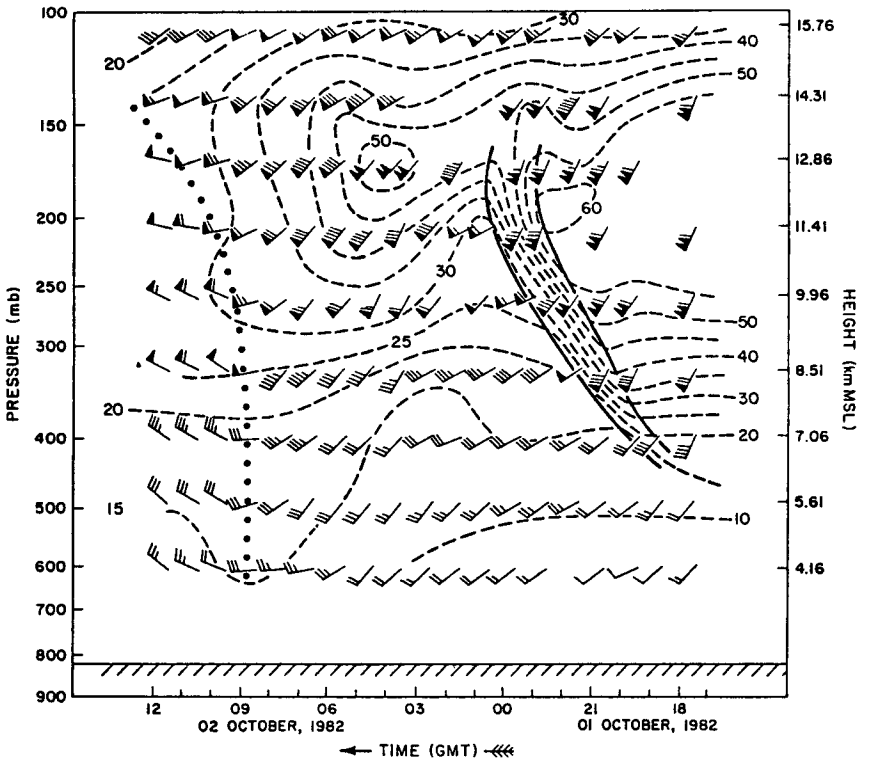


FIG. 10. Data sample from the VHF radar at Platteville (from Shapiro *et al.*, 1983). Wind vectors: flag = 25 m $s^{-1}$; full barb = 5 m $s^{-1}$; half barb = 2.5 m $s^{-1}$. Heavy dotted line is trough axis; solid lines are upper-level frontal boundaries; dashed lines are isotachs.

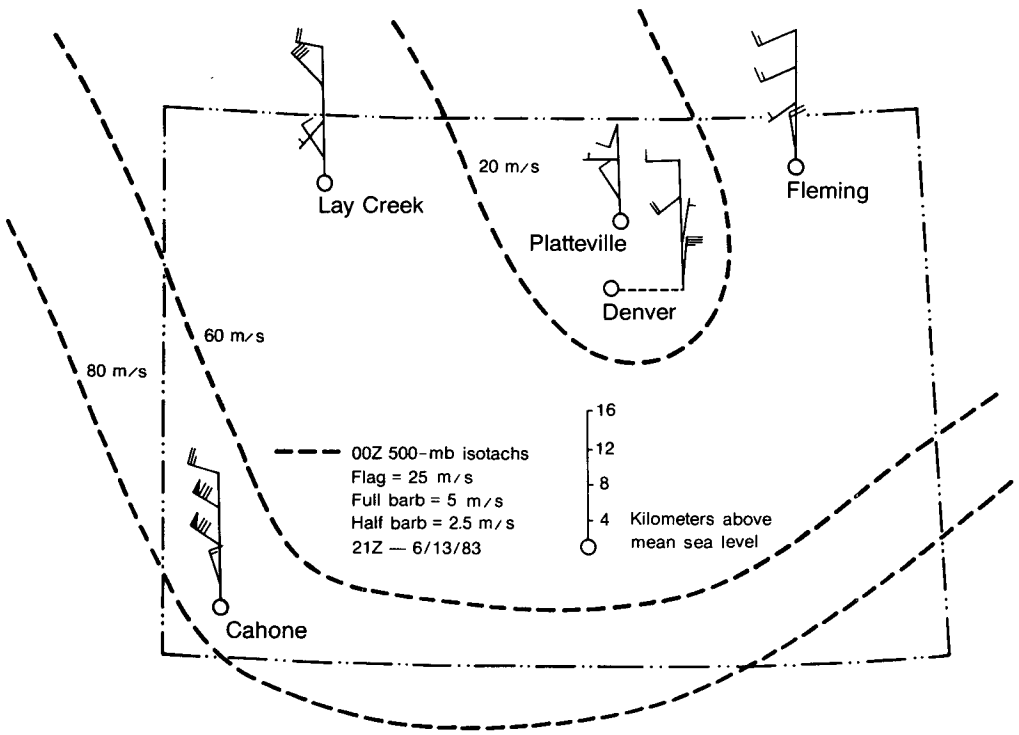


FIG. 11. Data sample from the Profiler radars. In this example only the Cahone radar observed the jet stream winds at 2100 GMT. The dashed lines show the 500 mb isotachs 3 h later.

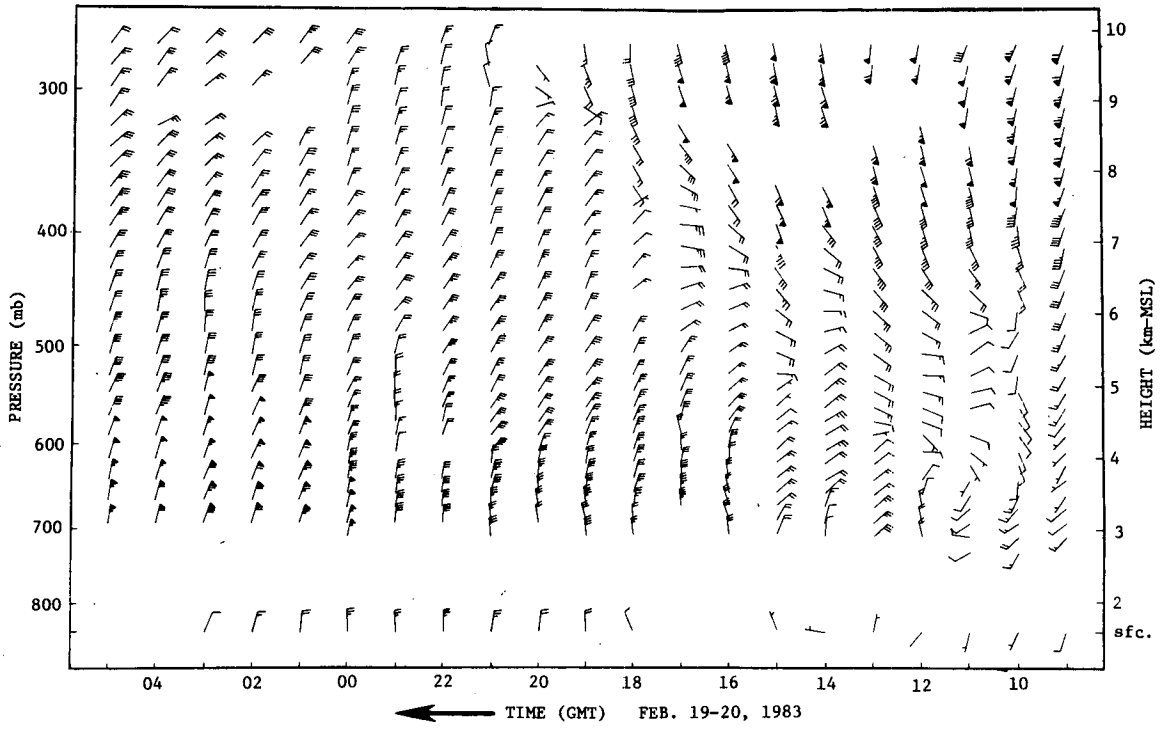


FIG. 12. Data sample from the UHF radar at Denver-Stapleton. Measured data points were available every 30 min; hourly profiles are plotted. Likewise, the number of measured points in each profile is about twice the number plotted.

is available, where the inertial subrange should allow measurements to above the tropopause, and where the antenna and transmitter costs are about the same as for VHF radars.

## 7. Conclusions

During the past decade research Doppler radar systems have demonstrated that vertical profiles of the horizontal wind can be measured in both the optically clear atmosphere and in precipitation. Radar, therefore, may be able to supply atmospheric wind data continuously and automatically for research and operational meteorology. We have constructed a network of five radars in Colorado to provide wind profiles for evaluation by meteorologists. These radars have many of the characteristics that would be desired in an operational network such as automated operation and remote control. After operating this network for an extended period (at least 1 year) we will be able to evaluate the capability of various types of radar wind profilers in a wide variety of meteorological conditions. We will then be able to specify the characteristics of a radar for measuring wind profiles in various research or operational applications or networks.

*Acknowledgments.* The long-wavelength radar techniques that we have utilized were pioneered in the Atmospheric Dynamics Program of ERL's Aeronomy Laboratory. In particular, the assistance and cooperation of Dr. Ben Balsley, Warner Ecklund, Dave Carter and Tony Riddle are gratefully acknowledged. We thank Mildred Birchfield for the preparation of this manuscript.

## REFERENCES

Atlas, D. A., R. C. Srivastava and R. S. Sekhon: 1973. Doppler radar characteristics of precipitation at vertical incidence. *Rev. Geophys. Space Phys.*, **11**, 1–35.

Balsley, B. B., and K. S. Gage, 1982: On the use of radars for operational wind profiling. *Bull. Amer. Meteor. Soc.*, **63**, 1009–1018.

Carlson, H. C., Jr., and N. Sundararaman, 1982: Real-time jetstream tracking: National benefit from an (S-T) radar network for measuring atmospheric motions. *Bull. Amer. Meteor. Soc.*, **63**, 1019–1026.

Carter, D. A., 1982: Private communication. Aeronomy Laboratory, NOAA/ERL, Boulder.

Earnshaw, K. B., D. C. Hogg and R. G. Strauch, 1982: A triple-beam antenna for wind-profiling radar. NOAA TM-ERL-WPL-108, NOAA Environ. Res. Labs., Boulder, 23 pp.

Ecklund, W. L., D. A. Carter and B. B. Balsley, 1979: Continuous measurement of upper atmospheric winds and turbulence using a VHF radar: Preliminary results. *J. Atmos. Terr. Phys.*, **41**, 983–994.

Fischler, M. A., and R. C. Bolles, 1981: Random sample consensus: A paradigm for model fitting with applications to image analysis and automated cartography. *Commun. Assoc. Comput. Mach.*, **24**, 381–395.

Frisch, A. S., and S. F. Clifford, 1974: A study of convection capped by a stable layer using Doppler radar and acoustic echo sounders. *J. Atmos. Sci.,* **31,** 1622–1628.

Hildebrand, P. H., and R. S. Sekhon, 1974: Objective determination of the noise level in Doppler spectra. *J. Appl. Meteor.,* **13,** 808–811.

Hill, R. J., 1978: Spectra of fluctuations in refractivity, temperature, humidity, and the temperature-humidity cospectrum in the inertial and dissipation ranges. *Radio Sci.,* **6,** 953–961.

Hogg, D. C., M. T. Decker, F. O. Guiraud, K. B. Earnshaw, D. A. Merritt, K. P. Moran, W. B. Sweezy, R. G. Strauch, E. R. Westwater and C. G. Little, 1983: An automatic profiler of the temperature, wind, and humidity in the atmosphere. *J. Climate Appl. Meteor.,* **22,** 807–831.

Labitt, M., 1981: Coordinated radar and aircraft observations of turbulence. Proj. Rep. ATC 108, MIT Lincoln Laboratory, 39 pp.

Nathanson, F. E., 1969: *Radar Design Principles.* McGraw Hill, 626 pp.

Ottersten, H., 1969: Atmospheric structure and radar backscattering in clear air. *Radio Sci.,* **4,** 1179–1193.

Röttger, J., 1980: Reflection and scattering of VHF radar signals for atmospheric refractivity structures. *Radio Sci.,* **15,** 259–276.

Schmidt, G., R. Ruster and P. Czechowsky, 1979: Complementary code and digital filtering for detection of weak VHF radar signals from the mesosphere. *IEEE Trans. Geosci. Electron.,* **GE-17,** 154–161.

Shapiro, M. A., D. C. Hogg and C. G. Little, 1983: The Wave Propagation Laboratory profiler system and its applications. *Preprints 5th Symp. Meteorological Observations and Instrumentation,* Toronto, Amer. Meteor. Soc., 174–182.

Strauch, R. G., M. T. Decker and D. C. Hogg, 1983: Automated profiling of the troposphere. *J. Aircraft,* **20,** 359–362.

Whalen, A. D., 1971: *Detection of Signals in Noise.* Academic Press, 411 pp.

Zrnić, D. S., 1979: Estimation of spectral moments for weather echoes. *IEEE Trans. Geosci. Electron.,* **GE-17,** 113–128.